Journal of Organometallic Chemistry, 166 (1979) 179—192

PREPARATION AND STRUCTURAL CHARACTERIZATION OF $[(\eta^5\text{-}C_5H_5)_2Zr(SC_6H_5)]_2O$. A QUALITATIVE DESCRIPTION OF THE BONDING IN OXO-BRIDGED DICYCLOPENTADIENYL-TRANSITION METAL DIMERS

JEFFREY L. PETERSEN

Department of Chemistry, West Virginia University, Morgantown, West Virginia 26506 (U.S.A.)

(Received July 18th, 1978)

Summary

The hydrolysis of $(\eta^5\text{-}C_5H_5)_2Zr(SC_6H_5)_2$ was shown previously by IR spectroscopy to produce an oxo-bridged complex. The molecular structure of this material has been determined by X-ray diffraction methods and consists of two $(\eta^2\text{-}C_5H_5)_2Zr(SC_6H_5)$ units linked by an oxo bridge. The Zr—O—Zr bond is nonlinear at 165.8(2)° with a Zr···Zr interatomic separation of 3.902(1) Å. The two independent S—Zr—O bond angles of 98.7(1) and 103.3(1)° are consistent with a d^0 electronic structure for each zirconium atom. The relatively short Zr—O distances of 1.968(3) and 1.964(3) Å support the presence of partial double-bond character arising from the donation of electron density from filled p_π-orbitals on the oxygen atom to unfilled d-orbitals on the electron deficient d^0 metal atoms. This bonding feature requires based upon orbital symmetry arguments that the $(ML)_2O$ molecular core in $[(\eta^5\text{-}C_5H_5)_2ML]_2O$ complexes must be nonplanar with a dihedral angle between the two L—M—O planes less than 90°. For $[(\eta^5\text{-}C_5H_5)_2Zr(SC_6H_5)]_2O$, a dihedral angle of 61.7° was observed. The compound crystallizes in an orthorhombic space group, *Pbca*, with refined lattices parameters a 16.458(4), b 20.281(5), and c 17.016(4) Å. Full-matrix least-squares refinement of 2613 diffractometry data with $I > \sigma(I)$ led to a final discrepancy index $R(F_0^2) = 0.044$.

Introduction

The synthesis of the mercaptide derivatives of $(\eta^5\text{-}C_5H_5)_2MCl_2$ (M = Ti, Zr, Nb) [1—3] is accomplished generally by reaction of the metallocene dichloride with stoichiometric amounts of RSH (R = alkyl or aryl substituent) and triethylamine. Although the reactions are rapid and produce high yields, the stability of the corresponding mercaptide product $(\eta^5\text{-}C_5H_5)_2M(SR)_2$ varies considerably.

Whereas the titanium complexes are generally air-stable, the zirconium analogues appear to be susceptible to hydrolysis and formation of coordination polymers [2]. Also, the presence of air or moisture during the preparation of $(\eta^5\text{-}C_5H_5)_2Zr(SR)_2$ has been shown by IR spectroscopic measurements to lead to the formation of a stable oxo-bridged zirconium species of unknown structure. An investigation into the formation of the oxo-bridged species has led to the isolation and subsequent structural characterization of $[(\eta^5\text{-}C_5H_5)_2Zr(SC_6H_5)]_2O$. The results of the X-ray diffraction study are presented as well as a qualitative description of the bonding in $[(\eta^5\text{-}C_5H_5)_2ML]_2O$-type complexes.

Experimental

Reagents

Dicyclopentadienylzirconium dichloride was prepared by published methods [4]. Triethylamine and the solvents were dried using normal techniques and distilled under a N_2 atmosphere. The Schlenk glassware was flame dried before use.

Analysis

Microanalyses were performed by Galbraith Laboratories, Inc., Knoxville, Tennessee.

Preparation of $[(\eta^5\text{-}C_5H_5)_2Zr(SC_6H_5)]_2O$

1.0 g (3.4 mmol) of $(\eta^5\text{-}C_5H_5)_2ZrCl_2$ was dissolved in 20 ml of benzene. Consecutive additions of 10 ml benzene solutions containing 0.75 g (6.8 mmol) of thiophenol and 0.69 g (6.7 mmol) of triethylamine produced a bright yellow solution of $(\eta^5\text{-}C_5H_5)_2Zr(SC_6H_5)_2$ [2]. The yellow solution was filtered and the excess solvent removed under vacuum. The resulting bright yellow solid was washed several times with hexane, dried, and then redissolved in benzene. Upon slow evaporation under a stream of nitrogen, pale yellow crystals, which were shown by X-ray diffraction analysis to be $[(\eta^5\text{-}C_5H_5)_2Zr(SC_6H_5)]_2O$ rather than $(\eta^5\text{-}C_5H_5)_2Zr(SC_6H_5)_2$, began to form on the side of the Schlenk tube. After approximately a week the yellow color of the solution diminished with the formation of more of the oxo-bridged dimer. Approximately 0.5 g (0.7 mmol) of the crystalline solid was isolated after removal of the remaining solution. The pale-yellow solid is insoluble in benzene and other common solvents and apparently is formed by the reaction of $(\eta^5\text{-}C_5H_5)_2Zr(SC_6H_5)_2$ with trace amounts of H_2O in the nitrogen stream. When the reaction was repeated with a moist nitrogen stream, the formation of the oxo-bridged dimer from the hydrolysis of $(\eta^5\text{-}C_5H_5)_2Zr(SC_6H_5)_2$ was completed within several hours. However, only an insoluble residue (rather than a crystalline sample) of the product could be obtained. The IR spectrum of the residue was identical to that of $[(\eta^5\text{-}C_5H_5)_2Zr(SC_6H_5)]_2O$.

Reaction of $(\eta^5\text{-}C_5H_5)_2Zr(SC_6H_5)_2$ with dry air

To a benzene solution of $(\eta^5\text{-}C_5H_5)_2Zr(SC_6H_5)_2$, which was prepared in the same manner as described earlier, air was admitted through a drying tube filled with Aquasorb attached to the side arm of the Schlenk tube. The yellow color of the solution also diminished with the formation of an insoluble residue, which

was isolated (0.25 g) and examined spectroscopically. The infrared spectrum of the solid, A, resembles that of $[(\eta^5\text{-}C_5H_5)_2ZrCl]_2O$ and is indicative of an oxo-bridged compound. However, the chemical analysis of A (C, 44.8; H, 3.8; O, 4.5; S, 0%) did not show the presence of any sulfur, in agreement with the noticeable absence of any phenylmercaptide absorption bands in the infrared spectrum. The elucidation of the structure of A awaits the isolation of suitable crystals for X-ray diffraction analysis.

Infrared spectra

Infrared spectra (calibrated with polystyrene film) were measured with a Beckman IR-8 spectrometer from KBr discs. The absorption spectra of $[(\eta^5\text{-}C_5H_5)_2ZrCl]_2O$, $[(\eta^5\text{-}C_5H_5)_2Zr(SC_6H_5)]_2O$, and solid A (obtained from the reaction of dry air with a solution of $(\eta^5\text{-}C_5H_5)_2Zr(SC_6H_5)_2$) were measured to aid in the characterization of reaction products.

For $[(\eta^5\text{-}C_5H_5)_2ZrCl]_2O$: 3120w, 1625(br), 1438m, 1360vw, 1015m, 1000(sh), 835(sh), 805st, 770m, 740st. For solid A: 3120w, 1590, 1540m, 1015st, 830 830(sh), 805st, 795(sh), 775m, 740st. For $[(\eta^5\text{-}C_5H_5)_2Zr(SC_6H_5)]_2O$: 3102m, 3078m, 1580m, 1480st, 1465m, 1440st, 1365m, 1085m, 1060m, 1020st, 1010st, 1000(sh), 840(sh), 825(sh), 815(sh), 805(sh), 800st, 790m, 760w, 740st, 715(sh), 705st, 690st, 665(sh).

Data collection

A pale-yellow, rectangular crystal of $[(\eta^5\text{-}C_5H_5)_2Zr(SC_6H_5)]_2O$ with dimensions of 0.20 × 0.20 × 0.25 mm was selected for the X-ray diffraction analysis. The crystal was mounted with epoxy on the end of a thin-glass fiber with the *a*-axis nearly parallel to the spindle axis of the goniometer and shown by preliminary oscillation and Weissenberg photographs to possess Laue symmetry D_{2h}-2/*m* 2/*m* 2/*m*. The observed systematic absences for $\{0kl\}$ of $k = 2n + 1$, for $\{h0l\}$ of $l = 2n + 1$, and for $\{hk0\}$ of $h = 2n + 1$ are compatible with only one centrosymmetric orthorhombic space group, *Pbca* (D_{2h}^{15}, No. 61).

The crystal was then aligned on a Picker four-circle automated diffractometer such that the intensity of the 800 reflection at χ 90° did not vary upon rotation of ϕ. The angular coordinates (χ, ϕ, and 2θ) of 24 strong diffraction peaks (2θ range 16—33°) were centered carefully by hand with Mo-K_α (λ 0.71069) radiation and least-squares refined to yield the final lattice parameters (Table 1). The least-squares refinement of the lattice parameters and the calculation of the orientation matrix and diffractometer angles were done using a modified version of PICKLIST, which was kindly supplied by Professor R. Doedens, University of California (Irvine).

A complete set of independent intensity data (*hkl*) was collected within a Bragg angle range $5° \leqslant 2\theta \leqslant 45°$. The data were measured at a take-off angle of 2.0° via $\theta - 2\theta$ scans from 0.65° below the $K_{\alpha 1}$ (λ 0.70926) 2θ setting to 0.65° above $K_{\alpha 2}$ (λ 0.71354) with a fixed scan rate of 2.0°/min. The diffracted beam was attenuated automatically by a previously calibrated attenuator when the counting rate exceeded 9000 counts/sec during the scan. (Stationary-crystal)—(stationary-counter) background counts of 10 sec were made on each side of a peak. The counter aperture of 1.0 mm diameter was placed 12 mm from the crystal. Zirconium-filtered Mo-K_α radiation was employed with a scintillation

TABLE 1

UNIT CELL AND SPACE GROUP DATA FOR $[(\eta^5\text{-}C_5H_5)_2Zr(SC_6H_5)]_2O$

Crystal System	Orthorhombic
a	16.458(4) Å
b	20.281(5) Å
c	17.016(4) Å
Volume	5672(3) Å^3
Density (obsd.)	1.563 g/cm^3
Density (calcd.)	1.548 g/cm^3
Z	8
μ	8.88 cm^{-1}
Range of transmission	0.82—0.86
Space group	*Pbca*
Systematic absences	$\{0kl\}$ $k = 2n + 1$
	$\{h0l\}$ $l = 2n + 1$
	$\{hk0\}$ $h = 2n + 1$

counter and pulse height analyzer adjusted to admit 90% of the Mo-K_α peak.

During data collection the intensities of two standard reflections were measured after every 50 reflections to monitor the instrument's stability as well as the crystal's alignment and decay. The variation in their intensities was no greater than 3%. After the data was corrected for background, absorption [6], and Lorentz-polarization effects, the values for I and $\sigma(I)$ were calculated for the 3909 measured reflections and averaged for duplicate reflections. The standard deviation for each corrected intensity was calculated from the expression

$$\sigma(I) = (S + B(t_s/t_b)^2 + E\,I^2)^{1/2}$$

where S designates the total integrated scan count accumulated in time t_s, B the total background count in time t_b, E an empirical factor of 0.0016, and I the integrated intensity equal to $S - B(t_s/t_b)$. Of the 3602 independent reflections, a total of 2613 reflections were considered observed with $I \geqslant \sigma(I)$. No corrections for extinction were necessary.

Solution and refinement of the structure

The crystal structure of $[(\eta^5\text{-}C_5H_5)_2Zr(SC_6H_5)]_2O$ was solved by conventional heavy-atom methods. The initial positions of the two independent zirconium atoms were obtained from an analysis [7] of the strongest peaks from a three-dimensional Patterson map; the coordinates for all of the remaining nonhydrogen atoms were revealed from subsequent Fourier syntheses. Full-matrix, anisotropic least-squares refinement with fixed atom contributions [8] for the cyclopentadienyl and phenyl hydrogen atoms led to final values for the discrepancy indices of $R(F_o) = 0.031$, $R(F_o^2) = 0.044$, and $R_w(F_o^2) = 0.059$ for all of the "observed" data. The least-squares refinements of the X-ray diffraction data were based on the minimization of $\Sigma\omega_i|F_o^2 - S^2F_c^2|$ where the individual weights, ω_i, equal $1/\sigma^2(F_o^2)$ and S is the scale factor. The discrepancy indices were calculated from the expressions

$$R(F_o) = [\Sigma||F_o| - |F_c||/\Sigma|F_o|] ,$$

$$R(F_o^2) = \Sigma|F_o^2 - F_c^2|/\Sigma F_o^2 , \text{ and}$$

$$R_w(F_o^2) = [\Sigma\omega_i|F_o^2 - F_c^2|^2/\Sigma\omega_i F_o^4]^{1/2}$$

(continued on p. 185)

TABLE 2

POSITIONAL PARAMETERS AND TEMPERATURE FACTORS FOR $[(\eta^5\text{-}C_5H_5)_2Zr(SC_6H_5)]_2O$ [a,b,c]

A. Positional parameters

Atom	x	y	z
Zr(1)	0.21471(3)	−0.00154(3)	0.09536(3)
Zr(2)	0.35856(3)	0.13813(3)	0.16965(3)
S(1)	0.08736(9)	0.06800(7)	0.07879(8)
S(2)	0.36790(9)	0.22750(7)	0.06428(8)
O	0.29225(20)	0.06955(16)	0.11933(18)
C(1)	0.1630(4)	−0.0032(3)	0.2381(3)
C(2)	0.1128(4)	−0.0464(3)	0.1959(3)
C(3)	0.1596(4)	−0.1001(3)	0.1701(3)
C(4)	0.2395(4)	−0.0898(3)	0.1966(3)
C(5)	0.2415(4)	−0.0307(3)	0.2393(3)
C(6)	0.2426(5)	0.0054(3)	−0.0510(3)
C(7)	0.3098(4)	−0.0236(4)	−0.0199(4)
C(8)	0.2870(6)	−0.0846(5)	0.0084(4)
C(9)	0.2040(6)	−0.0927(4)	−0.0073(4)
C(10)	0.1766(4)	−0.0365(4)	−0.0439(3)
C(11)	0.2230(3)	0.1699(3)	0.2297(3)
C(12)	0.2593(4)	0.2287(3)	0.2061(3)
C(13)	0.3271(4)	0.2395(3)	0.2534(4)
C(14)	0.3328(4)	0.1873(3)	0.3065(3)
C(15)	0.2697(4)	0.1430(3)	0.2902(3)
C(16)	0.4536(4)	0.0402(3)	0.1788(6)
C(17)	0.4834(4)	0.0783(5)	0.1187(4)
C(18)	0.5130(4)	0.1366(4)	0.1495(5)
C(19)	0.4981(4)	0.1353(4)	0.2294(5)
C(20)	0.4609(4)	0.0754(5)	0.2477(4)
C(21)	0.1036(3)	0.1166(3)	−0.0069(3)
C(22)	0.1661(4)	0.1608(3)	−0.0119(3)
C(23)	0.1779(4)	0.2000(3)	−0.0778(4)
C(24)	0.1237(4)	0.1943(3)	−0.1403(4)
C(25)	0.0599(4)	0.1503(3)	−0.1351(4)
C(26)	0.0500(3)	0.1116(3)	−0.0698(3)
C(27)	0.4268(3)	0.2003(3)	−0.0165(3)
C(28)	0.4956(4)	0.2329(3)	−0.0387(4)
C(29)	0.5402(4)	0.2219(4)	−0.1026(5)

B. Temperature factors

Atom	β_{11}	β_{22}	β_{33}	β_{12}	β_{13}	β_{23}	B (Å^2)
Zr(1)	309(2)	149(1)	194(2)	−14(2)	2(2)	−3(2)	
Zr(2)	257(2)	173(2)	233(2)	0(2)	−27(2)	3(2)	
S(1)	325(7)	263(5)	258(6)	0(5)	1(5)	49(4)	
S(2)	394(8)	207(5)	328(6)	−11(5)	55(6)	28(4)	
O	310(16)	179(11)	246(14)	−11(11)	−16(13)	−2(10)	
C(1)	467(33)	210(18)	220(23)	−39(22)	82(23)	27(19)	
C(2)	446(31)	173(19)	279(25)	−74(20)	12(23)	37(17)	
C(3)	527(36)	192(19)	283(24)	−94(21)	−66(27)	41(18)	
C(4)	447(34)	258(22)	382(29)	45(23)	17(26)	69(20)	
C(5)	518(35)	300(21)	186(23)	−104(24)	−77(24)	71(19)	
C(6)	622(38)	262(22)	220(23)	−18(27)	123(26)	−33(20)	
C(7)	445(38)	421(31)	408(34)	85(27)	132(29)	−90(25)	
C(8)	898(55)	407(32)	349(32)	385(37)	54(38)	−41(26)	
C(9)	1034(58)	193(23)	338(32)	−121(33)	251(38)	−101(22)	
C(10)	539(38)	369(27)	226(27)	−75(27)	−36(25)	−130(22)	
C(11)	253(28)	248(20)	315(26)	−2(19)	58(23)	−61(18)	
C(12)	398(31)	247(22)	308(25)	53(21)	69(25)	−31(18)	
C(13)	452(33)	232(20)	368(28)	−58(21)	110(26)	−78(21)	
C(14)	600(39)	282(22)	219(25)	−9(24)	−8(24)	−75(20)	
C(15)	590(36)	206(19)	229(23)	−20(23)	48(25)	−35(18)	
C(16)	438(36)	239(23)	782(45)	112(22)	−140(39)	54(30)	
C(17)	292(34)	566(35)	495(38)	134(28)	−70(29)	−123(32)	
C(18)	265(29)	465(30)	575(41)	7(26)	−14(28)	134(30)	
C(19)	343(33)	429(29)	588(43)	44(28)	−243(31)	−95(30)	
C(20)	422(37)	525(32)	427(34)	123(30)	−106(30)	151(32)	
C(21)	298(27)	172(18)	295(25)	8(18)	19(22)	32(17)	
C(22)	309(30)	312(23)	379(29)	2(21)	−64(24)	75(21)	
C(23)	352(31)	286(23)	594(36)	−58(21)	24(29)	142(24)	
C(24)	512(38)	374(25)	379(31)	6(26)	77(29)	176(23)	
C(25)	469(35)	463(29)	332(28)	−122(26)	−90(26)	113(24)	
C(26)	378(32)	351(23)	306(26)	−67(21)	−76(25)	96(21)	
C(27)	383(31)	228(20)	296(25)	−32(20)	23(24)	23(18)	
C(28)	483(35)	350(25)	465(31)	−141(25)	104(30)	0(23)	
C(29)	514(40)	562(35)	489(39)	−23(31)	243(34)	75(30)	

(Table continued)

TABLE 2 (continued)

A. Positional parameters

Atom	x	y	z
C(30)	0.5185(6)	0.1575(5)	−0.1438(4)
C(31)	0.4512(5)	0.1247(4)	−0.1228(4)
C(32)	0.4041(4)	0.1453(3)	−0.0603(4)
H(1)	0.1430	0.0390	0.2620
H(2)	0.0530	−0.0400	0.1850
H(3)	0.1390	−0.1380	0.1390
H(4)	0.2860	−0.1200	0.1860
H(5)	0.2880	−0.0100	0.2670
H(6)	0.2440	0.0510	−0.0740
H(7)	0.3650	−0.0050	−0.0180
H(8)	0.3250	−0.1160	0.0340
H(9)	0.1690	−0.1320	0.0060
H(10)	0.1200	−0.0270	−0.0630
H(11)	0.1730	0.1500	0.2070
H(12)	0.2380	0.2580	0.1630
H(13)	0.3660	0.2770	0.2500
H(14)	0.3740	0.1830	0.3490
H(15)	0.2610	0.1000	0.3170
H(16)	0.4300	−0.0050	0.1730
H(17)	0.4840	0.0660	0.0620
H(18)	0.5400	0.1720	0.1190
H(19)	0.5080	0.1720	0.2670
H(20)	0.4460	0.0600	0.3010
H(21)	0.2020	0.1650	0.0340
H(22)	0.2250	0.2310	−0.0800
H(23)	0.1270	0.2220	−0.1890
H(24)	0.0220	0.1450	−0.1800
H(25)	0.0030	0.0800	−0.0680
H(26)	0.5150	0.2720	−0.0080
H(27)	0.5890	0.2380	−0.1200
H(28)	0.5520	0.1400	−0.1890
H(29)	0.4340	0.0850	−0.1540
H(30)	0.3540	0.1200	−0.0470

B. Temperature factors

Atom	β_{11}	β_{22}	β_{33}	β_{12}	β_{13}	β_{23}	B (Å^2)
C(40)	658(49)	646(44)	326(35)	219(38)	132(35)	−7(30)	
C(31)	839(54)	478(33)	346(34)	116(35)	−69(35)	−220(27)	
C(32)	398(32)	319(24)	453(31)	−97(23)	−17(27)	−46(24)	
H(1)							5.0
H(2)							5.0
H(3)							5.0
H(4)							5.0
H(5)							5.0
H(6)							5.0
H(7)							5.0
H(8)							5.0
H(9)							5.0
H(10)							5.0
H(11)							5.0
H(12)							5.0
H(13)							5.0
H(14)							5.0
H(15)							5.0
H(16)							5.0
H(17)							5.0
H(18)							5.0
H(19)							5.0
H(20)							5.0
H(21)							5.0
H(22)							5.0
H(23)							5.0
H(24)							5.0
H(25)							5.0
H(26)							5.0
H(27)							5.0
H(28)							5.0
H(29)							5.0
H(30)							5.0

[a] The estimated standard deviations in parentheses for this and all subsequent tables refer to the least significant figure. [b] The form of the anisotropic temperature factor is $\exp\{-(\beta_{11}h^2 + \beta_{22}k^2 + \beta_{33}l^2 + 2\beta_{12}hk + 2\beta_{13}hl + 2\beta_{23}kl)\}$. [c] The components of the anisotropic temperature factor for each atom have been multiplied by 10^5.

TABLE 3

INTERATOMIC DISTANCES (Å) AND BOND ANGLES (deg) FOR $[(C_5H_5)_2Zr(SC_6H_5)]_2O$

A. Bond Distances			
Zr(1)—O	1.968(3)	Zr(2)—O	1.964(3)
Zr(1)—S(1)	2.542(2)	Zr(2)—S(2)	2.554(2)
S(1)—C(21)	1.780(6)	S(2)—C(27)	1.770(6)
Zr(1)—C(1)	2.574(5)	Zr(2)—C(11)	2.536(6)
Zr(1)—C(2)	2.564(6)	Zr(2)—C(12)	2.535(6)
Zr(1)—C(3)	2.537(6)	Zr(2)—C(13)	2.556(6)
Zr(1)—C(4)	2.517(6)	Zr(2)—C(14)	2.568(6)
Zr(1)—C(5)	2.559(5)	Zr(2)—C(15)	2.521(6)
Zr(1)—C(6)	2.535(5)	Zr(2)—C(16)	2.532(7)
Zr(1)—C(7)	2.549(7)	Zr(2)—C(17)	2.540(8)
Zr(1)—C(8)	2.538(9)	Zr(2)—C(18)	2.566(6)
Zr(1)—C(9)	2.551(7)	Zr(2)—C(19)	2.513(7)
Zr(1)—C(10)	2.552(6)	Zr(2)—C(20)	2.494(8)
B. Bond Angles			
S(1)—ZR(1)—O	98.7(1)	S(2)—Zr(2)—O	103.3(1)
C(21)—S(1)—Zr(1)	105.9(2)	C(27)—S(2)—Zr(2)	110.9(2)
C(22)—C(21)—S(1)	121.8(4)	C(28)—C(27)—S(2)	121.2(5)
C(26)—C(21)—S(1)	119.7(4)	C(32)—C(27)—S(2)	121.2(5)
Zr(1)—O—Zr(2)	165.8(2)		
C. Some interatomic contacts less than 4.0 Å about the central $(ZrS)_2O$ core			
Zr(1)···C(21)	3.480(5)	Zr(2)···C(27)	3.589(5)
S(1)···O	3.442(4)	S(2)···O	3.562(4)
Zr(1)···Zr(2)	3.902(1)		

The final goodness-of-fit parameter, $\sigma_1 = [\Sigma\omega_i|F_0^2 - F_c^2|/(n-p)]^{1/2}$ where n is the number of observations and p is the number of parameters varied (viz. 334), was 0.70, which indicates a small overestimation in the standard deviation of an average observation of unit weight. A final Fourier difference map revealed no unusual regions of residual electron density and thereby substantiates the correctness of the final structural model.

The positional and thermal parameters obtained from the last least-squares refinement cycle are presented in Table 2 for $[(\eta^5\text{-}C_5H_5)_2Zr(SC_6H_5)]_2O$ *. Interatomic distances and angles (with their estimated standard deviations calculated from the variance—covariance matrix) for the nonhydrogen atoms are provided in Table 3. The least-squares planes defined by specific atoms along with perpendicular displacements of these and other atoms from the planes and the dihedral angles between these planes were calculated. The scattering factors utilized in all structure factor calculations were those of Cromer and Mann [9] for the nonhydrogen atoms and those of Stewart et al. [10] for the hydrogen atoms with corrections included for anomalous dispersion effects [11] for the

* The table of structure factors and the equations for least-squares planes has been deposited as NAPS Document No. 03355 (18 pages). Order from ASIS/NAPS, c/o Microfiche Publications, P.O. Box 3513, Grand Central Station, New York, N.Y. 10017. A copy may be secured by citing the deposit number, remitting $ 5.00 for photocopies of $ 3.00 for microfiche. Advance payment is required. Make checks payable to Microfiche publications.

Zr and S atoms. The computer programs which were used in performing the necessary calculations for the X-ray diffraction data with their accession names in the World List of Crystallographic Computer Programs (Third Edition) are as follows: data reduction and absorption, DATALIB; data averaging and sort, DATASORT; Fourier summation, CNTFOR, modification of FORDAP; least-squares refinement, OR XFLS3; error analysis of distances and angles, OR FFE3; and structural drawing, OR TEP II. Least-squares planes were calculated with the program PLNJO based upon the method of Blow [12].

Results and discussion

Description of the molecular structure

The molecular configuration of $[(\eta^5\text{-}C_5H_5)_2Zr(SC_6H_5)]_2O$ (shown stereographically in Fig. 1) consists of two nearly identical $(\eta^5\text{-}C_5H_5)_2Zr(SC_6H_5)$ molecular units linked together by an oxo-bridge. The oxo-bridge occupies one of

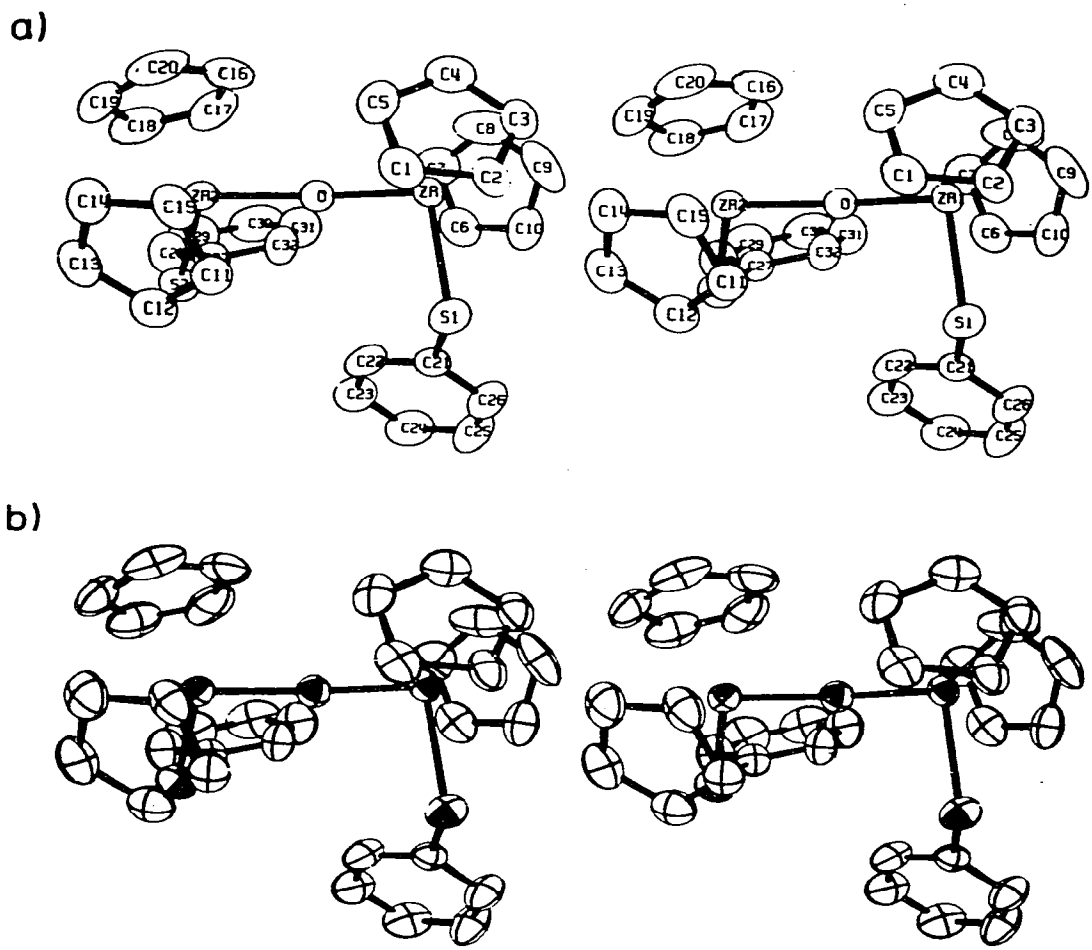

Fig. 1. Stereoscopic drawings of the molecular configuration of $[(\eta^5\text{-}C_5H_5)_2Zr(SC_6H_5)]_2O$ showing (a) the atom labeling and (b) the thermal ellipsoids for all nonhydrogen atoms scaled to enclose 50% probability.

four metal coordination sites and with the phenylmercaptide and the two centroids of the cyclopentadienyl rings completes a pseudotetrahedral arrangement around each Zr atom. A comparison of the corresponding interatomic distances and bond angles within the two independent $(\eta^5\text{-}C_5H_5)_2Zr(SC_6H_5)$ molecular groups reveals that the electronic environments around the Zr atoms are similar. As depicted for the $(ZrS)_2O$ core in Fig. 2, the two Zr—S (Zr(1)—S(1), 2.542(2) Å; Zr(2)—S(2), 2.554(2) Å) and two Zr—O (Zr(1)—O, 1.968(3) Å; Zr(2)—O, 1.964(3) Å) bond distances are essentially equivalent with the Zr—O—Zr bridging angle being 165.8(2)°. Each of the cyclopentadienyl rings are planar within 0.02 Å. The Zr—C distances systematically vary within the range of 2.49—2.58 Å around each of the rings and thereby indicate that the normal from each of the planar rings to the corresponding Zr atom is displaced from the ring centroid. The cyclopentadienyl C—C bond distances and C—C—C bond angles typically range from 1.37 to 1.41 Å and 1.07—110°, respectively. In contrast to $(\eta^5\text{-}C_5H_5)_2ML_2$-type (M = Ti, V; L = Cl^-, $SC_6H_5^-$) [1,14b] complexes in which the two cyclopentadienyl rings are symmetrically disposed with respect to the ML_2 fragment, the dihedral angles between each S—Zr—O plane and the corresponding cyclopentadienyl planes vary by ca. 6° in $[(\eta^5\text{-}C_5H_5)_2\text{-}Zr(SC_6H_5)]_2O$. This small angular tipping primarily serves to reduce some of the steric strain introduced by the unsymmetrical ligand environment around each Zr atom and the nonlinearity of the Zr—O—Zr linkage. The phenyl mercaptide ligands are planar with experimentally determined C—C bond distances which range from 1.34 to 1.39 Å and bond angles near 120°.

The only major difference in the two $(\eta^5\text{-}C_5H_5)_2Zr(SC_6H_5)$ molecular units is the ca. 5° difference in the two S—Zr—O bond angles of 98.7(1) and 103.3(1)°. For mononuclear $(\eta^5\text{-}C_5H_5)_2ML_2$ compounds the corresponding L—M—L bond angles for d^0, d^1, and d^2 systems have been found [1,13—16] to range from 94—105°, 85—94°, and 76—82°, respectively. Extrapolation of these results to the two S—Zr—O bond angles in $[(\eta^5\text{-}C_5H_5)_2(SC_6H_5)]_2O$ indicates that these bond angles are consistent with a d^0 zirconium(IV) configuration on each metal. Since the electronic environments around the Zr atoms are similar, the observed

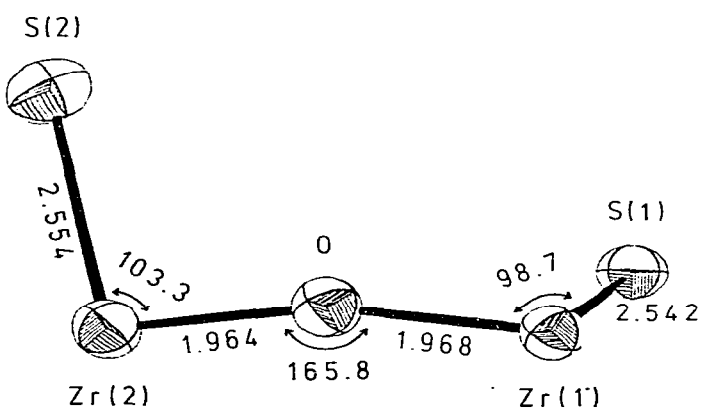

Fig. 2. Central $(ZrS)_2O$ molecular fragment with experimentally determined bond distances and bond angles.

ca. 5° difference in the two S—Zr—O bond angles is probably due to a combination of steric and packing effects.

Comparison with other oxo-bridged dimers

Structural studies, which have been performed on a variety of oxo-bridged dimers including the $[(MCl_5)_2O]^-$ monoanion (M = Ru, Os, W) [17—19], acetylacetonate derivatives such as $[Ti(acac)_2Cl]_2O$ [20] and cyclopentadienyl complexes such as $[(\eta^5\text{-}C_5H_5)TiCl_2]_2O$ [21,22], $\{[(\eta^5\text{-}C_5H_5)_2Ti(H_2O)]_2O\}(ClO_4)_2 \cdot 2\,H_2O$ [23], and $[(\eta^5\text{-}C_5H_5)_2ZrCl]_2O$ [24], have shown that the geometry of the M—O—M linkage can adopt either a linear or slightly bent configuration. For comparison purposes, the important structural features associated with known oxo-bridged cyclopentadienyl systems of Ti, Zr, and Nb are presented in Table 4. In both the Ti and Zr complexes the observed M—O distances are significantly shorter than the corresponding single bond distances for the Ti—O and Zr—O bonds of ca. 2.0 and 2.2 Å, respectively. These large differences strongly support the presence of partial double-bond character arising from the donation of electron density from filled p_π-orbitals on the oxygen atom to unfilled *d*-orbitals of the electron deficient d^0 metals (vide infra). A similar result has been observed for $[Ti(acac)_2Cl]_2O$ [20] in which the Ti—O bond distances for the bridging O atom of 1.79(2) and 1.81(2) Å are significantly shorter than the Ti—O bond distances for the σ-bonded acac ligands which vary from 1.91 to 2.07 Å. In all of the oxo-bridge systems listed in Table 4, the O—M—L bond angles reflect the d^0 electronic configuration of the metal atoms. Note that the two O—Zr—Cl bond angles in $[(\eta^5\text{-}C_5H_5)_2ZrCl]_2O$ differ in a manner similar to that observed for the phenylmercaptide derivative.

For the few oxo-bridged cyclopentadienyl compounds for which structural data is available, the M—O—M bond angle varies from a linear structure in a $[(\eta^5\text{-}C_5H_5)ML_2]_2O$-type complex to a slightly bent configuration (165—176°) in the $[(\eta^5\text{-}C_5H_5)_2ML]_2O$-type dimers. These structural differences are due to a composite of electronic and steric effects. For the oxo-bridged dimers which contain the smaller Ti atom, interring repulsions would be expected to have a greater influence on the M—O—M structure as evidenced by the nearly linear Ti—O—Ti structure of the $\{[(\eta^5\text{-}C_5H_5)_2Ti(H_2O)]_2O\}^{2+}$ cation [24]. Although these repulsions apparently are not sufficient to force a linear Ti—O—Ti linkage, they may help to explain the observed Ti—O bond distance of 1.829(2) Å, which is ca. 0.5 Å longer than that observed for $[(\eta^5\text{-}C_5H_5)TiCl_2]_2O$. In the case of $[(\eta^5\text{-}C_5H_5)TiCl_2]_2O$ these interactions are minimized by the crystallographically-imposed center of symmetry which maximizes the separation between the symmetry-related cyclopentadienyl rings. Preliminary results from a X-ray diffraction study [25] of $[(\eta^5\text{-}C_5H_5CH_3)_2ZrCl]_2O$ suggest that interring repulsions can perturb the central Zr_2Cl_2O configuration. Although no appreciable change in the Zr—O—Zr bond angle of ca. 170° is observed, the dihedral angle between the two Cl—Zr—O planes is increased by nearly 10° over that found in $[(\eta^5\text{-}C_5H_5)_2ZrCl]_2O$ [24]. This additional steric hindrance provided by the methyl substituents is also sufficient to force the methylcyclopentadienyl rings to rotate away from their normal positions (as found in $(\eta^5\text{-}C_5H_4CH_3)_2MCl_2$, M = Ti [14b], Zr [26]) such that the methyl groups are directed away from one another. Although the basic structure of the $(ML)_2O$ core of these oxo-

bridged dimers is relatively rigid and appears to be dictated primarily by electronic factors, minor structural modifications can arise from steric interactions between cyclopentadienyl rings, which become more significant as the size of the metal atom is reduced or as substituents on the rings are introduced.

Another characteristic structural feature associated with the $[(\eta^5\text{-}C_5H_5)_2ML]_2O$ complexes in Table 4 is the acute dihedral angle between the two L—M—O molecular planes. This feature is shown for $[(\eta^5\text{-}C_5H_5)_2Zr(SC_6H_5)]_2O$ in Fig. 3, which depicts a view of the molecule nearly along the Zr···Zr direction. The observed dihedral angle of 61.7° between the two S—Zr—O planes in $[(\eta^5\text{-}C_5H_5)_2Zr(SC_6H_5)]_2O$ is smaller than the corresponding angles in $[(\eta^5\text{-}C_5H_5)_2ZrCl]_2O$ and $\{[(\eta^5\text{-}C_5H_5)_2NbCl]_2O\}^{2+}(BF_4^-)_2$. Figure 3 also shows that a consequence of the acute dihedral angle is the coordination of the two mercaptide ligands to the same side of the molecule. This structural feature is a general one for $[(\eta^5\text{-}C_5H_5)_2ML]_2O$ complexes and suggests that it may be possible to coordinate a bidentate ligand simultaneously to both metal atoms.

Qualitative bonding description for $[(\eta^5\text{-}C_5H_5)_2ML]_2O$ dimers

A qualitative understanding of the bonding in $[(\eta^5\text{-}C_5H_5)_2ML]_2O$ dimers can be obtained by consideration of the idealized representation of the orbital overlap region (as depicted in Fig. 4) for the $(ML)_2O$ core. This representation, which for illustration purposes assumes a linear M—O—M structure, is based upon the results of several theoretical and experimental studies [13,14] of the electronic structure of $(\eta^5\text{-}C_5H_5)_2ML_2$-type complexes. From these investiga-

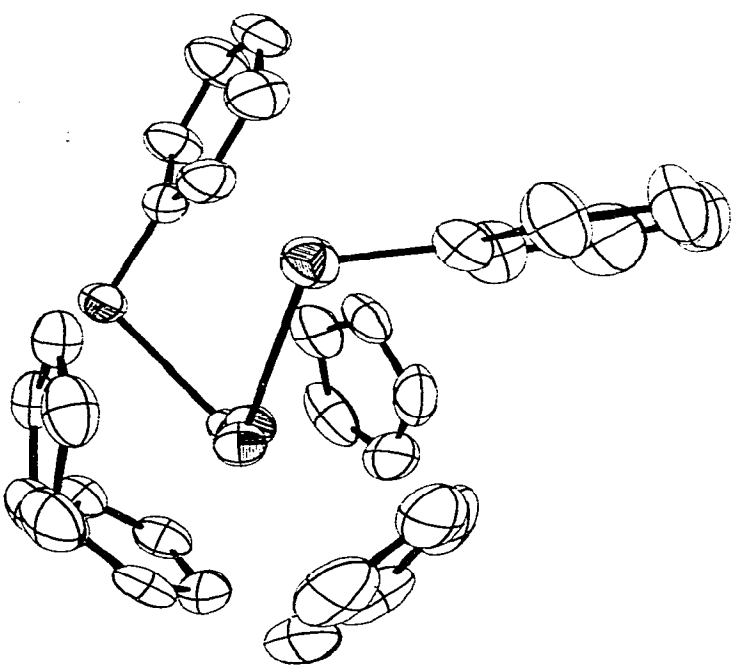

Fig. 3. View of the $[(\eta^5\text{-}C_5H_5)_2Zr(SC_6H_5)]_2O$ molecule approximately along the Zr···Zr direction. The dihedral angle between the two S—Zr—O planes is 61.7°.

TABLE 4

X-RAY STRUCTURAL DATA FOR KNOWN OXO-BRIDGED CYCLOPENTADIENYL-TRANSITION METAL DIMERS

Ref.	Compound	Crystal type	Z	M—O (Å)	O—M—X (deg) [a]	M—O—M (deg) [a]	Dihedral angle [b]
21	$[(\eta^5\text{-}C_5H_5)TiCl_2]_2O$	Monoclinic, $P2_1/c$	2	1.78(3)	104(2)	180	—
22	$[(\eta^5\text{-}C_5H_5)TiCl_2]_2O$	Monoclinic, $P2_1/n$	2	1.777(1)	102.3 103.1	180	
23	$\{[(\eta^5\text{-}C_5H_5)_2Ti(H_2O)]_2O\}(ClO_4)_2 \cdot 2\ H_2O$	Orthorhombic, $Fdd2$	8	1.829(2)	94.3(3)	175.8(5)	74.1
24	$[(\eta^5\text{-}C_5H_5)_2ZrCl]_2O$	Monoclinic, $C2$	4	1.94(1) 1.95(1)	99.3(3) 96.8(5)	168.9(8)	74.3
25	$[(\eta^5\text{-}C_5H_4CH_3)_2ZrCl]_2O$	Orthorhombic, $Pbca$	8				
This work	$[(\eta^5\text{-}C_5H_5)_2Zr(SC_6H_5)]_2O$	Orthorhombic, $Pbca$	8	1.968(3) 1.964(3)	98.7(1) 103.3(1)	165.8(2)	61.7
16	$\{([(\eta^5\text{-}C_5H_5)_2NbCl]_2O\}^{2+}(BF_4^-)_2$	Orthorhombic, $Pnn2$	2	1.88(1)	96.2(9)	169.3(8)	72.5

[a] X represents the monodentate ligand (H_2O, Cl^-, or $SC_6H_5^-$) bonded to the metal atom in these oxo-bridged dimers. [b] The dihedral angle made by the two O—M—X planes.

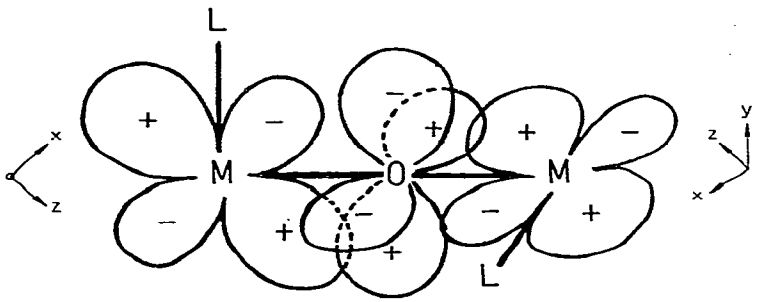

Fig. 4. An idealized representation of the orbital overlap for the interaction of the filled oxygen p_π-orbitals with the unfilled metal a_1 d-orbitals. Coordinate systems are defined separately for each metal. The diagram assumes the L—M—O bond angles are 90°, the dihedral angle between the two L—M—O planes is 90°, and the M—O—M bond is linear.

tions the LUMO in the corresponding d^0 complexes (where M = Ti, or Zr) was shown to be primarily d_{z^2} in character with a small but significant contribution from the $d_{x^2-y^2}$ orbital (based upon a Cartesian coordinate system on M with the x-axis bisecting the L—M—L bond angle and the y-axis normal to the ML_2 plane). The electronic configuration of the metal has an appreciable effect on the magnitude on the L—M—L bond angle and the M—L bond distance. In general, as the number of the nonbonding electrons on the metal increases, the L—M—L bond angle decreases from a d^0 (Ti, Zr) to d^1 (V, Nb) to d^2 (Mo) system with an accompanying increase in the M—L bond length. Since the spatial distribution of the LUMO of a_1 symmetry in the mononuclear d^0 systems is directed normal to the plane which bisects the L—M—L bond angle, the corresponding hybrid orbital on each metal in the oxo-bridged dimer has the correct symmetry to overlap with one of the fill oxygen p_π-orbitals. The resultant π-donation from these filled oxygen AO's to the empty metal orbitals provides a reasonable explanation for the significantly shorter M—O bonds observed for the oxo-bridged dimers which have been structurally characterized. This bonding representation contrasts that proposed for $\{(\eta^5\text{-}C_5(CH_3)_5)_2ZrN_2\}_2N_2$ [27], where the electron density is donated from the filled a_1 orbital of the two d^2 Zr atoms to the π^*-acceptor orbitals of the bridging dinitrogen ligand. However, in both systems, the bonding interaction between the bridging ligand and the metals requires the dihedral angle between the two L—M—O planes in the oxo-bridged dimers or between the two N—Zr—N planes (i.e., 87°) in $\{(\eta^5\text{-}C_5(CH_3)_5)_2ZrN_2\}_2N_2$ be near 90°. Consequently, the possibility of a planar $(ML)_2O$ (or $(ZrL)_2N_2$) core is ruled out.

For a bond angle near 90°, one expects (based solely upon electronic factors) to observe a 90° dihedral angle between the two L—M—O planes and a linear M—O—M linkage. However, the d^0 electronic configuration associated with each metal in $[(\eta^5\text{-}C_5H_5)_2Zr(SC_6H_5)]_2O$ and other related dimers is characterized by L—M—O bond angles which are significantly greater than 90°. Qualitatively, an increase in the L—M—O bond angle will improve the overlap of each unfilled metal orbital with the corresponding oxygen p_π-orbital However, this structural variation to the idealized representation in Fig. 4 introduces some degree of destabilization since a small antibonding contribution from the interaction of the metal orbital with the other oxygen p_π-orbital is possible. This effect

increases in importance as the L—M—O bond angles becomes more obtuse but can be minimized by a simultaneous reduction in the bridging angle from 180° and the dihedral angle between the two L—M—O planes from 90°. Although limited structural data are available for $[(\eta^5\text{-}C_5H_5)_2ML]_2O$ complexes, the structural parameters given in Table 4 are consistent with this correlation.

From this qualitative bonding representation the electronic configuration of the metal (as reflected by the size of the L—M—O bond angle) plays an important rcle in determining the magnitude of the M—O—M bond angle and the dihedral angle between the two L—M—O planes in $[(\eta^5\text{-}C_5H_5)_2ML]_2O$ complexes. In the absence of additional steric effects introduced by a smaller metal atom such as Ti, substituents on the cyclopentadienyl rings, or bulky L ligands, orbital symmetry arguments suggest that the dihedral angle in these dimers cannot be greater than 90° and a linear M—O—M bond may be only possible when the L—M—O bond angle is near 90°. Therefore, one might expect that as the LUMO becomes occupied (as would be the case for d^1 and d^2 configurations) the accompanying decrease in the L—M—O bond angle would result in a more nearly linear M—O—M bond angle. The M—O bond distance should increase appreciably due to the electron—electron repulsions. Work is currently in progress to investigate the correlation between the electron configuration on the metal and the geometry of the $(ML)_2O$ fragment in these oxo-bridged dimers.

Acknowledgements

Acknowledgement is made to the donors of the Petroleum Research Fund, administered by the American Chemical Society, for support of this work. Computer time for the X-ray diffraction data analysis was provided by the West Virginia Network for Educational Telecomputing.

References

1 E.G. Muller, S.F. Watkins, and L.F. Dahl, J. Organometal. Chem., 111 (1976) 73.
2 H. Köpf, J. Organometal. Chem., 14 (1968) 353.
3 W.E. Douglas and M.L.H. Green, J. Chem. Soc. (Dalton), (1972) 1976.
4 J.J. Eisch and R.E. King, Organometallic Synthesis, Vol. 1, Academic Press, New York, 1965.
5 A.F. Reid, J.S. Shannon, J.M. Swan, and P.C. Wailes, Aust. J. Chem., 18 (1965) 173.
6 International Tables for X-ray Crystallography, Vol. III, Kynoch Press, Birmingham, 1968, p. 162.
7 J.C. Calabrese, PHASE, Ph.D. Thesis (Appendix II), University of Wisconsin, Madison, 1971.
8 J.C. Calabrese, MIRAGE, Ph.D. Thesis (Appendix III), University of Wisconsin, Madison, 1971.
9 D.T. Cromer and J. Mann, Acta Crystallogr. Sect. A, 24 (1968) 321.
10 R.F. Stewart, E.R. Davidson, and W.T. Simpson, J. Chem. Phys., 42 (1965) 3175.
11 D.T. Cromer and D. Liberman, J. Chem. Phys., 53 (1970) 1891.
12 D. Blow, Acta Crystallogr., 13 (1960) 168.
13 J.L. Lauher and R. Hoffmann, J. Amer. Chem. Soc., 18 (1976) 1729, and ref. cited therein.
14 (a) J.L. Petersen and L.F. Dahl, J. Amer. Chem. Soc., 96 (1974) 2248;
(b) J.L. Petersen and L.F. Dahl, ibid., 97 (1975) 6416, 6422;
(c) J.L. Petersen, D.L. Lichtenberger, R.F. Fenske, and L.F. Dahl, ibid., 97 (1975) 6433.
15 J.C. Green, M.L.H. Green, and C.K. Prout, Chem. Commun., (1975) 421 and ref. cited therein.
16 K. Prout, T.S. Cameron, R.A. Forder, S.R. Critchley, B. Denton, and G.V. Rees, Acta Crystallogr., Sec B, 30 (1974) 2290.
17 A.M. Mathieson, D.P. Mellor, and N.C. Stephenson, Acta Crystallogr., 5 (1952) 185.
18 K.F. Tebbe and H.G. von Schnering, Z. Anorg. Chem., 396 (1973) 66.
19 J. San Fillippo, Jr., R.L. Grayson, and H.J. Sniadoch, Inorg. Chem., 15 (1976) 269.
20 K. Watenpaugh and C.N. Caughlin, Inorg. Chem., 6, (1967) 963.
21 P. Corradini and G. Allegra, J. Amer. Chem. Soc., 81 (1959) 5510.
22 U. Thewalt and D. Schomburg, J. Organometal. Chem., 127 (1977) 169.
23 U. Thewalt and D. Schomburg, J. Organometal. Chem., 150 (1978) 59.
24 J.F. Clarke and M.B. Drew, Acta Crystallogr., Sect B, 30 (1974) 2267.
25 J.L. Petersen, work in progress.
26 J.L. Petersen, J.W. Egan, Jr., manuscript in preparation.
27 R.D. Sanner, J.M. Manriquez, R.E. Marsh, and J.E. Bercaw, J. Amer. Chem. Soc., 98 (1976) 8351.